Recombination of Three Atoms in the Ultracold Limit

B. D. Esry
Institute for Theoretical Atomic and Molecular Physics, Harvard-Smithsonian Center for Astrophysics, Cambridge, Massachusetts 02138

Chris H. Greene and James P. Burke, Jr.
Department of Physics and JILA, University of Colorado, Boulder, Colorado 80309-0440
(Received 19 May 1999)

We identify two qualitatively different mechanisms that control three-body recombination in a spin-polarized gas near zero temperature. A universal curve describes the recombination rate versus the two-body scattering length a. It grows as a^4 for large $|a|$, with different mechanisms for $a < 0$ and $a > 0$. Our calculations document a previously established mechanism that causes K_3 to grow rapidly as the two-body scattering length a increases toward $+\infty$, and a new tunneling mechanism that produces an even stronger enhancement of K_3 as $a \to -\infty$. The expectations based on these two mechanisms can be modified by quantum mechanical interference or resonance effects.

PACS numbers: 34.10.+x

Three-body recombination processes such as Rb + Rb + Rb $\to$ Rb_2 + Rb limit the density and lifetime of current generation Bose-Einstein condensates (BECs). Such processes are also important in nuclear physics and in chemical dynamics. Yet the current state of recombination theory remains primitive, compared to the highly successful scattering theory for two bodies. In perturbative regimes, the theory developed by Verhaar and coworkers [1–3] has been applied to collisions of three hydrogen atoms. The validity of such treatments for the alkalis, which interact far more strongly, is highly questionable.

Meanwhile, experimentalists recently created a Bose-Einstein condensate with tunable properties [4–6]. When a magnetic field B is applied near a diatomic Feshbach resonance, a condensate is created with a custom two-body scattering length $a(B)$. So far, however, the promise of a tunable BEC has been negated by a huge rise in the three-body recombination [7] that rapidly devours the condensate.

Fedichev *et al.* [8] predicted in 1996 that the low-energy recombination rate exhibits explosive growth with increasing scattering length a, namely $K_3^{\mathrm{FRS}} \simeq 23\frac{\hbar}{m}a^4$. Yet their derivation is valid only if $a > 0$ is large. Another theoretical study [9] suggested that the recombination rate should be even larger when $-a$ is equally large, because a negative scattering length lowers a barrier in the three-body entrance channel. This same effect ultimately destabilizes a many-atom BEC when $a < 0$ [10,11].

In this article we develop a comprehensive description of three-body recombination and show its key implications. First of all, we present a quantitative method that can be used to calculate numerically stable recombination rates when the two-body interactions are short range in character. Then, based upon many calculations, we identify two qualitatively different mechanisms for recombination. Both mechanisms, remarkably, cause K_3 to grow as a^4 for large $|a|$, but with a much larger coefficient when $a < 0$. This simple a^4 scaling can be modified, however, by a resonance or interference effect. We find in particular that three-body recombination losses should not generally prevent the formation of a tunable BEC.

Our formulation uses the framework of Delves [12], who showed that a *countable* set of three-body collision channels can still be defined at energies above the threshold for breakup ($E = 0$) using hyperspherical coordinates. In this representation, $\mathbf{S}$ is manifestly symmetric and unitary. The permutation symmetry is enforced using "democratic hyperspherical coordinates" (c.f. Ref. [13]). Further, we need only the $L = 0$ block of the scattering matrix since the generalization of Wigner's threshold law leads to $K_3 \propto E^L$ near threshold.

The derivation of our recombination rate expression in terms of the scattering matrix is too lengthy to convey here. In the ultracold limit, we obtain

$$\sigma_{\mathrm{identical}}^{\mathrm{recomb}} = \frac{1152\pi^2}{k^5}\,|\mathbf{S}_{A_2+A\leftarrow A+A+A}|^2. \qquad (1)$$

Here $k = (2\mu E/\hbar^2)^{1/2}$ is the hyperradial wave number in the incident three-body continuum channel, and $\mu = m/\sqrt{3}$ is the three-body reduced mass. This generalized cross section has units of (length)^5, as is appropriate to characterize radial scattered flux in 6 dimensions. We adopt the convention of Mott and Massey [14] in defining the cross section for identical particle collisions as the ratio of the scattered radial flux to the incident flux in *one* of the six symmetrizing permutations of the incident plane wave. Equation (1) leads to an energy-independent constant value for K_3 in the limit of infinitesimal incident energy. Our results confirm the approximate a^4 power law dependence predicted for large $a > 0$ in Ref. [8], although we find a larger coefficient. Our results are not consistent with the a^2 dependence predicted in Ref. [2].

The *event* rate constant is simply $K_3 = \frac{\hbar k}{\mu}\sigma_{\mathrm{identical}}^{\mathrm{recomb}}$ for recombination in a thermal gas of spin-polarized bosons.

For atoms in a BEC, this rate is reduced by a factor of 3!, a result predicted by theory [15] and observed experimentally [16]. For a mixture of condensed and noncondensed atoms, the factors have been discussed in Ref. [17]. Often the rate constant is quoted as an *atom-loss* rate constant, the coefficient of the density cubed in the rate equation. This quantity is $L_3 = 3K_3/6$, where the factor of 3 in front of K_3 arises because both the diatom and the final state atom are typically ejected from a trap following each recombination event. The division by 6 reflects the fact that there are $N^3/6$ atom triples in a fixed volume.

We solve coupled equations in an adiabatic hyperspherical representation [18] using the variational R-matrix method [19]. The short range two-body potentials permit us to extract the asymptotic S-matrix simply, without transforming to Jacobi coordinates at large hyperradius R as is usually done in reactive scattering calculations. It is necessary to integrate the coupled equations out to surprisingly large radii, $R > 10^4$ a.u., in order to extract a stable scattering matrix at these ultracold energies.

The interaction used is a sum of triplet two-body potentials, i.e., $v(r_{12}) + v(r_{23}) + v(r_{31})$. This choice is appropriate for fully spin-polarized atoms that collide in a quartet electronic spin state. By symmetry, precisely one hyperspherical potential curve of the trimer must converge asymptotically to each dimer bound state. An infinite set of potential curves associated with three-body entrance and exit channels must approach the three-body dissociation threshold ($U = 0$) asymptotically, but a generalized Wigner threshold law guarantees that scattering is dominated by the lowest three-body entrance channel at threshold.

In order to rapidly survey the dominant mechanisms, we have used model two-body potentials. One set of calculations scales the physical Rb-Rb triplet potential by an overall constant factor γ, $0 \le \gamma \le 1$, mimicking the experimental ability to tune the scattering length. This rescaling economizes the calculations substantially, since the total number of bound diatomic channels is reduced to a manageable number. We have also performed extensive calculations using $v(r_{12}) = D\,\mathrm{sech}^2(r_{12}/r_0)$, as in [9]. If the recombination rate is controlled only by the two-body scattering length a [8,9], this simplification should not matter. We further test this premise by treating two-body potentials that support different numbers of bound two-body channels but which generate the same scattering length.

Figure 1(a) shows the hyperspherical potential curves for the sech^2 potential scaled to give a two-body scattering length $a = 100$ a.u. approximately equal to the known ^{87}Rb triplet scattering length, but with only a single s-wave bound state. The potential curves are very simple for this case, and their main features are consistent with Refs. [9,18]. A distant avoided crossing between the three-body entrance channel and the highest s-wave recombination channel occurs generally near $R \simeq 3a$. The $a < 0$ case in Fig. 1(b) shows no such long-range

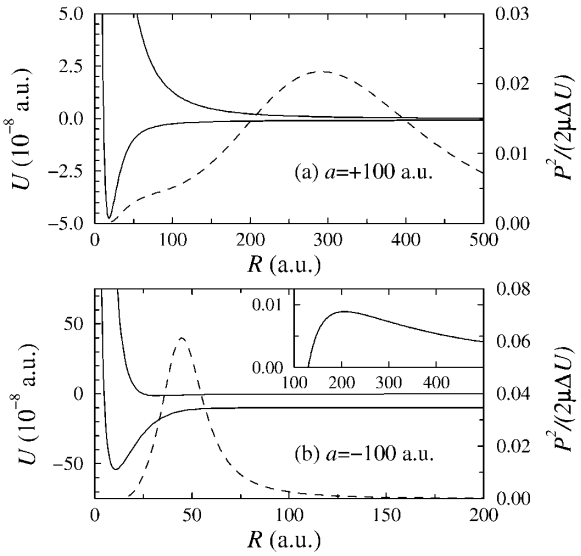

FIG. 1. The lowest two adiabatic hyperspherical potential curves (solid line) along with their nonadiabatic coupling strength (dashed line) for (a) $a > 0$ and (b) $a < 0$. The nonadiabatic coupling strength is a dimensionless quantity defined as the ratio of the squared coupling matrix element $P_{12}^2(R)$ to the product of the difference in the adiabatic potential curves $\Delta U(R)$ and the reduced mass μ. The inset in (b) shows the potential barrier in the three-body entrance channel.

avoided crossing, but a potential barrier in the three-body entrance channel at $R \simeq -2a$ has key implications discussed below.

Figure 2 shows our nonperturbative recombination calculations for over 80 different two-body potentials, including a wide range of scattering lengths and different numbers of two-body bound states. Figure 2 shows rates obtained using both the sech^2 two-body potential with $r_0 = 18.8$ a.u. and the rescaled Rb potential. This plot is presented in a new way that we find revealing [20], as a "recombination length" defined by

$$\varrho_3 = \left(\frac{\mu}{\hbar}\,K_3\right)^{1/4}.$$

This definition is intended to present a quantity largely independent of the atomic properties other than the scattering length, and to reduce to a number roughly comparable to the scattering length in magnitude. Here $\mu = \sqrt{m_1 m_2 m_3/(m_1 + m_2 + m_3)}$ is the three-body reduced mass, which reduces to $m/\sqrt{3}$ for three identical atoms.

Remarkably, the calculated rate constants in Fig. 2 cluster along a single universal curve, suggesting that the value of K_3 is controlled primarily by a. Figure 2 also shows two additional features that have apparently not been discussed in the literature previously, namely a shape resonance effect arising at $a \simeq -175$ a.u. and an interference minimum at $a \simeq 290$ a.u. The following two simple mechanisms explain these results qualitatively.

(i) Recombination at $a > 0$.—The primary recombination mechanism when a is large and positive involves a rather broad avoided crossing near $R \sim 3a$

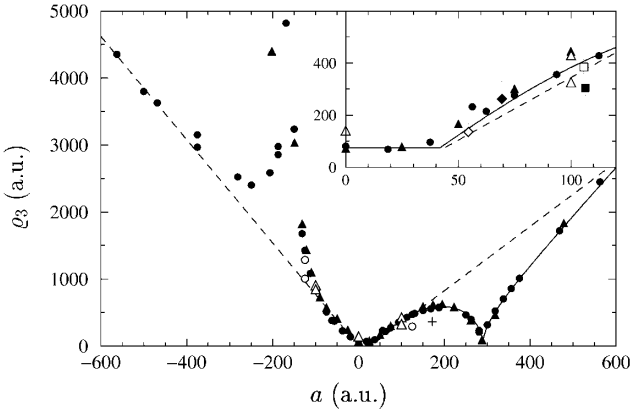

FIG. 2. Numerically calculated recombination lengths ϱ_3 for ultracold ^{4}He and spin-stretched ^{87}Rb are compared with Eq. (3) as a function of the scattering length a. The circles are for two-body sech^2 potentials with $r_0 = 18.8$, for one s-wave bound state (filled), and multiple s-wave states (open). Triangles show results obtained using a rescaled Rb potential, filled (one s-wave bound state) and open (multiple states). The + symbol is our result for helium, using a realistic potential. The solid curve is Eq. (3) with the $\sin^2\Phi$ Stückelberg factor, while the dashed curve uses its average value (1/2). The inset shows four experimental measurements, for Rb $|1,-1\rangle$ (filled square), Rb $|2,2\rangle$ (open square), Na $|1,-1\rangle$ (open diamond, $B = 0$), and Na $|1,1\rangle$ (filled diamond, $B = 894.5$ G), from Refs. [16,17,7,7], respectively. Calculations were performed at 1 μK, except for $a \leq -300$ a.u. which were calculated at 0.1 μK to reach the ultracold limit. For He, Na, K, and Rb, Eq. (3) agrees with our full calculations if the parameter r_0 is chosen to equal 9.4, 12.4, 16.9, and 18.8 a.u., respectively.

between the highest s-wave two-body channel and the lowest three-body channel [see Fig. 1(a)]. This mechanism is consistent with the qualitative scenario postulated in [8,9]. Whenever inelastic scattering occurs through such a Landau-Zener-type avoided crossing, the possibility arises for constructive or destructive interference between two competing pathways that contribute coherently—so-called "Stückelberg oscillations" [14,21].

At threshold, the scattering probability for the rate-limiting transition into the highest s-wave recombination channel behaves approximately as

$$|\mathbf{S}_{A_2+A\leftarrow A+A+A}|^2 \rightarrow 0.067(ka)^4 \sin^2\Phi\,, \quad a \rightarrow +\infty\,, \tag{2}$$

where Φ is the phase difference between the two pathways. A crude evaluation of Φ can be made by approximating the highest s-wave potential curve by the potential relevant in the Efimov limit of very large, positive a (see, e.g., [9]). This approximation yields $\Phi \simeq \ln(3a/2r_0)$ for the sech^2 potential where r_0 is a constant in the vicinity of 1–20 a.u. [The $\sin^2$ factor of Eq. (2) can likely be approximated by 1/2 in systems having numerous two-body bound states, because the returning wave is likely to be dissipated into other two-body channels by the many avoided crossings. This point requires additional study.]

(ii) Recombination at $a < 0$.—The rate-limiting step in this case is not a long-range avoided crossing as was found for $a > 0$. Rather, it is quantum mechanical tunneling under the barrier identified previously in [9], which in our present notation occurs at $R_{\text{barrier}} \simeq -2.0a$, with a barrier maximum of $U(R_{\text{barrier}}) \simeq 0.079/\mu a^2$, in a.u. [see Fig. 1(b)]. In physical terms, the incident three-body wave front near zero energy must tunnel inside this barrier in order to reach the avoided crossings with recombination channels which lie at much smaller radii.

Since the rate limiting step for $a < 0$ is a tunneling process, this suggests that a shape resonance in the three-body entrance channel potential can dramatically enhance the recombination rate at certain values of a. The condition for a zero energy resonance is simply the Bohr-Sommerfeld quantization condition for a quasibound state in the inner well of the three-body entrance curve. In the limit of very large negative values of a, this WKB integral is approximately the phase Φ calculated above for $a > 0$. The logarithmic dependence of the phase on $|a|$ implies that the zero-energy rate should be enhanced at an infinite number of Efimov-like shape resonances as a approaches $-\infty$. Experiments carried out at fixed, *nonzero* energy E, however, can only observe a finite number, because the barrier height decreases as $1/\mu a^2$ as $a \rightarrow -\infty$, and it eventually falls below E.

The calculated rates using $v(r_{ij}) = D\,\text{sech}^2(r_{ij}/r_0)$, for different values of r_0 can all be represented compactly by a single formula. While Eq. (2) gives a reasonable approximation, better agreement with our numerical rates is obtained using the following expression for the zero temperature recombination length (in a.u.):

$$\varrho_3^{\text{th}}(a) \simeq \max\begin{cases} 5.0(a - \frac{3}{2}r_0)\,[2\sin^2(\ln\frac{3a}{2r_0})]^{1/4}, & a > 0, \\ -7.7a, & a < 0, \\ 4r_0. \end{cases} \tag{3}$$

The slopes in this expression are accurate to about ±5%. Figure 2 confirms that this formula with $r_0 = 18.8$ a.u. agrees with our full numerical calculations for the rescaled ^{87}Rb potential with a single s-wave bound state. For other alkalis, see the values cited in the caption to Fig. 2, but note that the phase of the $\sin^2$ function may require adjustment. For helium, Eq. (3) with $r_0 = 9.4$ a.u. gives quantitative agreement with our numerical values; in particular, it places the interference minimum correctly at $a \simeq 145$ a.u. Equation (3) has a lower limit of $\varrho_3^{\text{th}} \simeq 4r_0$ because $\varrho_3^{\text{th}} \gtrsim 50$–$100$ a.u. in all of our numerical calculations. This effect is presumably due to other channels that become more important when the dominant channels weaken sufficiently. Any Stückelberg minimum can be vanishingly small, however, if just one recombination channel is present.

Table I compares our estimates based on Eq. (3) with experimental results presently available for spin-polarized collisions in various atoms, and with other theories. (For these estimates the Stückelberg $\sin^2$ factor was replaced by its average value 1/2.) The value shown for helium in Table I is from our full numerical calculation, however,

TABLE I. Recombination event rate constants for helium and for the alkalis.

Atom	a (a.u.)	Present K_3^{th} (cm^6/s)	Experiment K_3^{exp} (cm^6/s)	Other K_3^{th} (cm^6/s)
^{4}He	172	4.2×10^{-27}	...	2.5×10^{-27} [a]
^{7}Li	-27.6	2.5×10^{-28}	$<6 \times 10^{-27}$ [b]	5.2×10^{-28} [c]
^{23}Na$(1,-1)$	54.6	3.9×10^{-29}	1.3×10^{-29} [d]	4.4×10^{-30} [a]
^{23}Na$(1,1)$	69.5	1.6×10^{-28}	1.8×10^{-28} [d]	4.0×10^{-28} [c], 1.2×10^{-29} [a]
^{39}K	-33	9.2×10^{-29}	...	...
^{85}Rb	-370	6.7×10^{-25}	...	...
^{87}Rb$(1,-1)$	106	2.3×10^{-28}	9×10^{-29} [e]	8×10^{-30} [c]
^{87}Rb$(2,2)$	106	2.3×10^{-28}	2.2×10^{-28} [f]	1.7×10^{-29} [a]
^{133}Cs$(3,3)$	-1250	5.6×10^{-23}	$<10^{-23}$ [g]	1×10^{-28} [h]

[a][8] [b][22] [c][2] [d][7] [e][16] [f][17] [g][23] [h][3]

rather than from Eq. (3), since we can perform the calculation without rescaling the potential. Table I shows event rates per collision, K_3, rather than total atom loss rates L_3; experimental results reported as L_3 appropriately converted. Where recombination rates have been reported for atoms in a BEC [7,17], we have multiplied the measured rates by 6 to compare with our theoretical rates for ultracold noncondensed atoms.

The lone experiment that deviates from our predicted dependence of ϱ_3 on a (except at $a \geq 50$) is the magnetic field Feshbach resonance studied for Na. This might suggest that the mechanisms at work are different from those addressed here. If the recombination rates measured in [7] are plotted in the form $\varrho_3(a)$, they grow as a decreases from 50 a.u. toward 0 which we have never observed in our calculations. This behavior, if it is confirmed as a three-body process, probably signals the presence of a three-body Feshbach or shape resonance of an entirely different type than we have observed for stretched spin states. The theoretical rate for Cs in Table I is constant only below 0.1 μK, whereas the experimental bound from [23] was measured at 10 μK, where we estimate a rate lower by about 100.

In summary, we have developed a method to calculate quantitative three-body recombination rates for a spin-polarized atomic gas. A survey of over 120 different two-body potentials allowed us to identify the physical mechanisms relevant for different signs of a. Our results suggest a universal behavior as a function of a, namely a simple a^4 scaling, modified in some cases by quantum mechanical interference or shape resonance effects. In fact, the Na $|1,\pm1\rangle$ and Rb $|1,-1\rangle$ experiments cited in Table I do not involve the stretched spin states for the atoms involved but still agree with our calculations. While we suspect that many of our results are still applicable in this case, there are almost certain to be far more exceptions, owing to the more prevalent occurrence of three-body Feshbach and shape resonances. The resulting dynamical issues that arise in this more complicated regime of collisions will require much further study in the future.

This work was supported in part by the National Science Foundation. We thank J. Bohn, G. Bertsch, and P. Julienne for informative discussions. We also thank the authors of Ref. [7] for sending their experimental data in numerical form.

[1] See, for instance, L. P. H. de Goey *et al.*, Phys. Rev. B **38**, 646 (1988).
[2] A. J. Moerdijk and B. J. Verhaar, Phys. Rev. A **53**, R19 (1996); A. J. Moerdijk *et al.*, Phys. Rev. A **53**, 916 (1996).
[3] E. Tiesinga *et al.*, Phys. Rev. A **46**, R1167 (1992).
[4] S. Inouye *et al.*, Nature (London) **392**, 151 (1998).
[5] Ph. Courteille *et al.*, Phys. Rev. Lett. **81**, 69 (1998).
[6] J. L. Roberts *et al.*, Phys. Rev. Lett. **81**, 5109 (1998).
[7] J. Stenger *et al.*, Phys. Rev. Lett. **82**, 2422 (1999); see also D. M. Stamper-Kurn *et al., ibid.* **80**, 2027 (1998).
[8] P. O. Fedichev *et al.*, Phys. Rev. Lett. **77**, 2921 (1996).
[9] B. D. Esry *et al.*, J. Phys. B **29**, L51 (1996). Note that $\mu^{\text{present}} = (4/3)^{1/2}\mu^{\text{old}}$ and $R^{\text{present}} = (3/4)^{1/4}R^{\text{old}}$. See also Z. Zhen and J. H. Macek, Phys. Rev. A **38**, 1193 (1988).
[10] See the review by F. Dalfovo *et al.*, Rev. Mod. Phys. **71**, 463 (1999).
[11] J. L. Bohn *et al.*, Phys. Rev. A **58**, 584 (1998).
[12] L. M. Delves, Nucl. Phys. **9**, 391 (1958); **20**, 275 (1960).
[13] J. G. Frey and B. J. Howard, Chem. Phys. **99**, 415 (1985).
[14] N. F. Mott and H. S. W. Massey, *The Theory of Atomic Collisions* (Clarendon Press, Oxford, 1965), 3rd ed., pp. 294–300.
[15] Y. Kagan *et al.*, JETP Lett. **42**, 209 (1985).
[16] E. A. Burt *et al.*, Phys. Rev. Lett. **79**, 337 (1997).
[17] J. Söding *et al.*, Appl. Phys. B (to be published).
[18] B. D. Esry *et al.*, Phys. Rev. A **54**, 394 (1996); Hyperspherical methods are reviewed in C. D. Lin, Phys. Rep. **257**, 1 (1995).
[19] M. Aymar *et al.*, Rev. Mod. Phys. **68**, 1015 (1996).
[20] We thank P. Julienne for a conversation that led to this idea.
[21] H. Nakamura, Int. Rev. Phys. Chem. **10**, 123 (1991).
[22] J. M. Gerton *et al.*, Phys. Rev. A **59**, 1514 (1999).
[23] V. Vuletić *et al.*, Phys. Rev. Lett. **82**, 1406 (1999).